ORIGINAL PAPER

Comparison and integration of final electromagnetic stirring and thermal soft reduction on continuous casting billet

Yan-shen Han[1] · Wei Yan[1] · Jiang-shan Zhang[1] · Jun Chen[2] · Wei-qing Chen[1] · Qing Liu[1]

Abstract

Final electromagnetic stirring (F-EMS) and thermal soft reduction (TSR) are techniques that improve the inner quality of continuous casting billets, but they have rarely been applied simultaneously. The application effects of F-EMS and TSR were compared, and a process integrating F-EMS and TSR was adopted for a billet continuous caster. A heat transfer model was established to calculate the thermal behavior of 82A tire cord steel billet. The locations of F-EMS and TSR were determined, followed by conducting a series of plant trials, involving F-EMS alone, TSR alone, and the integrated process of F-EMS and TSR. The results showed that F-EMS or TSR could effectively improve the inner quality of the billet under their respective suitable working conditions. Moreover, F-EMS was found to be more helpful in terms of improving central segregation, while TSR tended to improve V-segregation, central porosity, and pipe. The integration of F-EMS and TSR allowed the advantages of each technique to be utilized, thereby better improving the inner quality. Among all the working conditions, 82A steel billet showed optimum inner quality when the current of F-EMS was 240 A and the cooling intensity of TSR was 2.2 $m^3 h^{-1}$. These findings demonstrate that the integration of F-EMS and TSR is promising for application on continuous casting billets.

Keywords Billet continuous casting · Final electromagnetic stirring · Thermal soft reduction · Central segregation · Inner quality

1 Introduction

The formation of segregation, porosity, and pipe is inevitable in continuous casting billets during the solidification process. The existence of these defects severely deteriorates the inner quality of the billets. To improve the inner quality, certain techniques such as mechanical soft reduction (MSR) [1, 2], mechanical heavy reduction [3, 4], final electromagnetic stirring (F-EMS) [5–7], final permanent magnetic stirring [8], and thermal soft reduction (TSR) [9–11] have been developed, and remarkable outcomes have been achieved. These techniques primarily act on the solidification end of the strands and have different mechanisms and advantages to improve the inner quality of the billets. Among these

techniques, F-EMS and soft reduction (SR) are most extensively used, and their effects on billets or blooms are frequently compared [12, 13]. F-EMS can promote the liquid flow and break the dendrite using an electromagnetic force, and therefore homogenizes the temperature and composition of the residual liquid and increases the equiaxed crystal ratio. SR can compensate for the central solidification shrinkage through a mechanical force (namely MSR) or an intensive water-spray cooling (namely TSR), and consequently, the inflow of enriched liquid can be prevented.

Presently, demand for continuous casting billets and blooms with high inner quality is increasing in light of higher requirements for product quality. It is challenging to achieve such high product-quality requirements by adopting just one technique. Therefore, as the installation positions of F-EMS and SR on continuous caster differ, these two techniques can be used simultaneously. Accordingly, F-EMS and MSR are integrated to improve the inner quality of the blooms, and it has been proven that their combination is more effective than using any one technique [14, 15]. For continuous casting billets, the application of MSR

✉ Qing Liu
 qliu@ustb.edu.cn

1 State Key Laboratory of Advanced Metallurgy, University of Science and Technology Beijing, Beijing 100083, China

2 Xiangtan Iron & Steel Co., Ltd. of Hunan Valin, Xiangtan 411101, Hunan, China

is not as effective as it is in the case for blooms, especially for high carbon steels [16]. Most billet continuous casters are mainly and only equipped with F-EMS. TSR has a similar effect as MSR and is an efficient technique for billets. Therefore, working with F-EMS seems to be a good choice for billet continuous casters, and the integration of F-EMS and TSR is worth investigating.

In the present study, both F-EMS and TSR were applied on a billet continuous caster. The comparison and integration of F-EMS and TSR were investigated on 82A tire cord steel billet. A heat transfer model was developed to calculate the thermal variation of the billet and determine the locations of F-EMS and TSR. Thereafter, a series of plant trials were conducted, including F-EMS alone, TSR alone, and the integration of F-EMS and TSR. The central segregation, V-segregation, central porosity, and pipe of the billets under different technological parameters were compared and discussed. Finally, the optimum parameters of F-EMS and TSR were determined for 82A steel billet.

2 Description of continuous casting process

2.1 Continuous caster

A 12-strand billet continuous caster was studied. The caster mainly produces the billets with a dimension of 150 mm × 150 mm. A schematic of the caster is shown in Fig. 1. The caster structurally includes the mold, the secondary cooling zone, and the air-cooling zone. The secondary cooling zone is divided into four segments with varying lengths. To improve the quality of the billet, the caster is equipped with mold electromagnetic stirring (M-EMS), F-EMS, and TSR. Both M-EMS and F-EMS can generate rotating magnetic fields and adopt a continuous stirring mode. In the secondary cooling zone and TSR zone, air-mist spraying nozzles are used to cool the billet.

2.2 Casting parameters

Table 1 lists the main chemical composition of 82A tire cord steel, which was obtained by analyzing liquid steel in the tundish. The main casting parameters of 82A steel are listed in Table 2. While casting, the casting parameters were steadily controlled as far as possible.
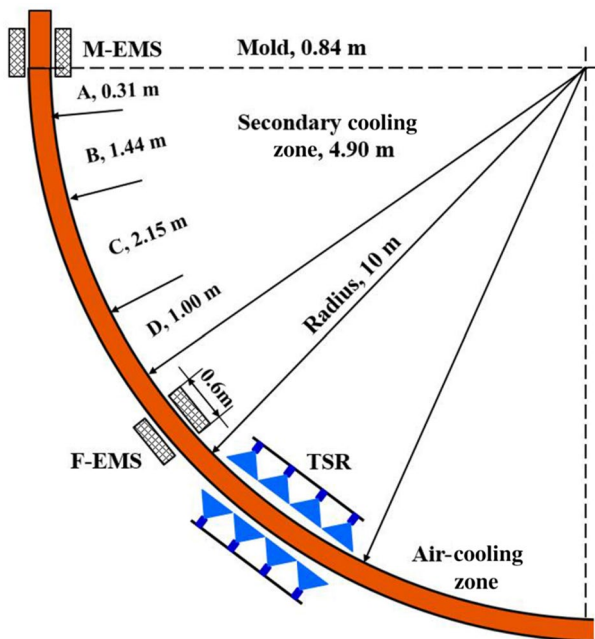

Fig. 1 Schematic illustration of caster

Table 2 Main casting parameters of 82A steel

Item	Value
Sectional dimension/(mm × mm)	150 × 150
Pouring temperature/°C	1488
Casting speed/(m min^{-1})	1.8
Water flux of mold cooling/(m^3 h^{-1})	125
Temperature difference between inlet and outlet of mold water/°C	7
Water flux of secondary cooling/(m^3 h^{-1})	9.05
Current of M-EMS/A	300
Frequency of M-EMS/Hz	4
Ambient temperature/°C	25
Water temperature/°C	35

Table 1 Main chemical composition of 82A steel (mass%)

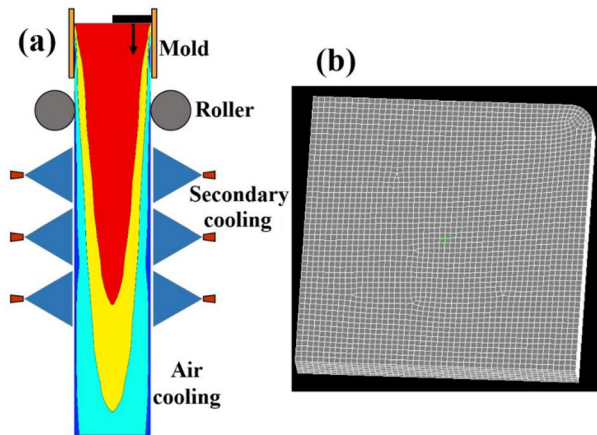| C	Si	Mn	P	S	Cr	Ni	Cu	Al	Ti	Fe
0.83	0.23	0.5	0.01	0.007	0.015	0.008	0.007	0.0017	0.0006	Balance

Fig. 2 Schematic illustration of slice moving method (**a**) and geometric model of slice (**b**)

3 Heat transfer model

A heat transfer model was established on the basis of a slice moving method. Figure 2 gives the schematic illustration of the slice moving method and the geometric model of the slice. A billet slice was adopted by considering the simplification of the calculation. The dimension of the slice was 75 mm × 75 mm × 10 mm. The slice also considered the round corner with a 6-mm radius. During simulation, it was assumed that the slice successively passed different cooling zones with varied boundary conditions. The detailed descriptions of the model, including the assumption, governing equation, boundary conditions, and the validation, are provided in our previous works [17, 18].

4 Locations of TSR and F-EMS

TSR is applied by exerting an intensive water-spray cooling on the steel surface at the solidification end of the billet. The objective of its application is to compensate for the solidification shrinkage of the central region and restrain the liquid flow toward the billet center [11, 19, 20]. Sivesson et al. [9, 10] reported that TSR should be located at the point where the central solid fraction was 0.2 until the billet completely solidified. In our previous study [18], the location of TSR was discussed. We found that TSR should start from the position where the central temperature of the billet begins to drop rapidly and ends at the liquid impenetrable temperature. The thermal behavior of the billet was calculated using the heat transfer model. Figure 3 depicts the variations of the central temperature and solid fraction of the billet. It can be observed that the central temperature of the billet rapidly decreases at approximately 6.96 m from meniscus and drops to the liquid impenetrable temperature at about 8.46 m from
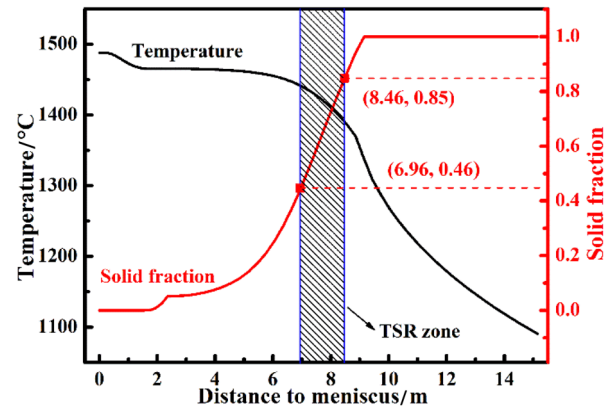

Fig. 3 Variations of central temperature and solid fraction of billet

meniscus. Therefore, TSR should be applied at a range of 6.96–8.46 m from meniscus.

The purpose of F-EMS is to apply an electromagnetic force to promote the flow of liquid steel and achieve certain metallurgical effects. The solid fraction of billet center and liquid pool thickness are normally used as the bases when determining the location of F-EMS, and these bases differ with respect to the steel grade and sectional dimension of the billet. For medium carbon steel billet with a dimension of 150 mm × 150 mm, Mizukami et al. [21] found that the optimum location of F-EMS lied in the point where the central solid fraction of the billet was 0.1. Oh and Chang [22] proposed that the optimum liquid pool thicknesses of S82 steel bloom (250 mm × 300 mm) and S72 steel billet (160 mm × 160 mm) were 54 and 55 mm, respectively. Jiang and Zhu [23] suggested that a stirring liquid pool thickness of 61 mm could better improve the central segregation of 0.82% C steel billet (160 mm × 160 mm) with the continuous stirring mode of F-EMS. The stirring liquid pool thickness of 61 mm was used to determine the location of F-EMS.

Figure 4 shows the variations of central solid fraction and shell thickness of the billet. The solidified shell is defined as the region where the solid fraction is 1. Correspondingly, the liquid pool refers to the region where the solid fraction is less than 1, including the liquid and mushy area. When TSR is not applied, the optimum position of F-EMS is 6.93 m from meniscus. As the length of F-EMS stirrer is 0.6 m, F-EMS is determined to locate at 6.63–7.23 m from meniscus, where the central solid fraction and liquid pool thickness vary from 0.37 to 0.51 and 64 to 56 mm, respectively. When TSR is applied, the potential location of F-EMS is in the range of 5.74–6.96 m from meniscus, and the initial determined location of F-EMS is identified to be conflicting with that of TSR. Considering the length of the F-EMS stirrer and the need of some space for convenient assembly, the location of F-EMS is determined to be 6.0–6.6 m from meniscus, and the corresponding central solid fraction and liquid pool thickness vary from 0.25 to
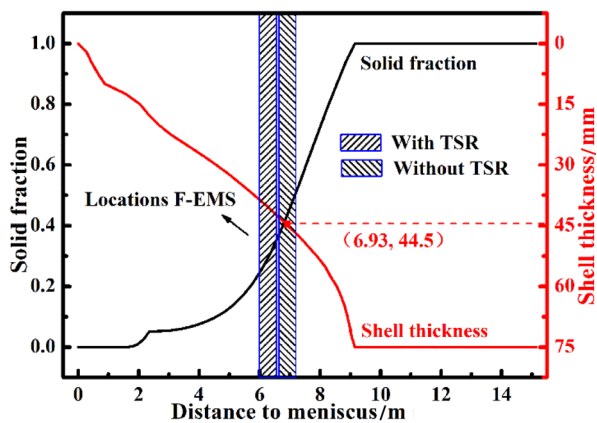
Fig. 4 Variations of central solid fraction and shell thickness of billet

0.36 and 72 to 64 mm, respectively. As the location of F-EMS needs to consider equipment restrictions, it is applied a little earlier than the optimum position when TSR is applied.

5 Experimental works

5.1 Industrial tests

A series of industrial tests were conducted to compare the inner quality of the billets under different F-EMS and TSR parameters. The adopted technological parameters are listed in Table 3. The currents of F-EMS varied from 180, 200, 220, 240, 260 to 280 A, and the cooling intensities of TSR varied from 0.87 to 2.2 m^3 h^{-1}. As it was difficult to maintain a steady current for F-EMS when it exceeds 280 A, the maximum current of F-EMS was set to 280 A. To prevent the potential internal and corner cracks caused by TSR, the maximum cooling intensity of TSR was set to 2.2 m^3 h^{-1}, which allowed the maintenance of a reasonable reheating rate and surface temperature. The frequency of F-EMS, secondary cooling intensity, and casting speed were 8 Hz, 0.5 L kg^{-1}, and 1.8 m min^{-1}, respectively, and they were relatively steadily controlled. The pouring temperature of each trial was approximately 1488 °C with a fluctuation no more than 5 °C. All the plant trials were performed on the eleventh strand. Trials 1 to 7 were carried out at the first cast, and trials 8 to 16 were performed at the secondary cast. The technological parameters were adjusted every 400 s during the trials,

and the corresponding billet samples were cut at a length of 500 mm.

5.2 Laboratory experiments

All the billet samples adopted from the plant trials were further treated to analyze the central segregation and macro-morphologies. For the analysis of central segregation, five successive transverse samples were sliced using a saw machine. The thickness of the sample was 20 mm. Both the sides of the samples were drilled to 10 mm depth at the center of the transverse section using alloy drillings, as shown in Fig. 5a. A carbon/sulfur analyzer was used to analyze the carbon content of the drills. The central segregation of the billet was represented using the central carbon segregation degree of the samples. The segregation degree was defined as C/C_0, where C is the carbon content of the drillings and C_0 is the carbon content of the liquid steel in the tundish. For analyzing macro-morphologies, transverse and longitudinal samples were cut using the saw machine, as shown in Fig. 5b. The detecting faces of the samples were polished using a grinding machine, and then eroded using hydrochloric acid solution for approximately 20 min. The concentration and the temperature of the solution were 50% and 70 °C, respectively. Thereafter, the samples were blow-dried and photographed to analyze the V-segregation, central porosity, and pipe.
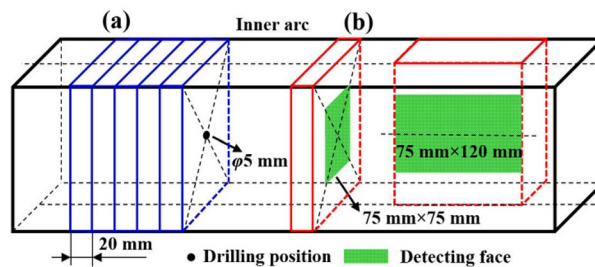

Fig. 5 Schematic diagram of sampling method for central segregation (**a**) and macro-morphologies (**b**)

Table 3 Technological parameters of F-EMS and TSR

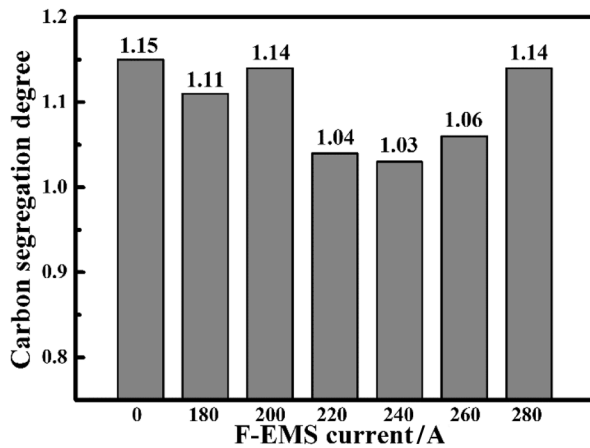| Trial number	1	2	3	4	5	6	7	8	9	10	11	12	13	14	15	16
F-EMS current/A	0	180	200	220	240	260	280	0	0	200	240	280	0	200	240	280
TSR cooling/(m^3 h^{-1})	0	0	0	0	0	0	0	0	0.87	0.87	0.87	0.87	2.2	2.2	2.2	2.2

Fig. 6 Average central carbon segregation degrees of billets with only F-EMS

6 Results and discussion

6.1 Comparison on central segregation

Figure 6 shows the average central carbon segregation degrees of the billets with only F-EMS. Without F-EMS, the average central carbon segregation degree is 1.15. The severe central segregation is significantly harmful to the billet quality. By applying F-EMS, the central segregation is effectively reduced, but the effect is not obvious at low currents (below 200 A). This indicates that the low F-EMS current has limited stirring ability and has small effect on central segregation improvement. When the current ranges from 200 to 240 A, F-EMS shows remarkable effects on central segregation. The average central carbon segregation degree decreases with the increase in F-EMS current, and reaches a minimum value of 1.03 at the current of 240 A. Thereafter, the central segregation exhibits an increasing trend with the increase in F-EMS current. When the F-EMS current is 280 A, the average central carbon segregation degree increases to 1.14. It indicates that excessive stirring is also harmful for the central segregation of the billet. Jiang et al. [23, 24] described a similar phenomenon, which can be explained using two mechanisms. One is the formation of negative segregation at the solidified front due to intense rotational flow, and therefore the positive segregation is aggravated at the billet center [25, 26]. The other is the formation of a low-pressure region near the center region of the billet, which could result in the inflow of the liquid phase, thus prolonging the solidification and enriching the solute elements at the billet center [24]. In a word, F-EMS could reduce the central segregation of the billet, but the stirring intensity needs to be controlled within a reasonable range. When the current of F-EMS ranges from 220 to 260 A, F-EMS shows positive effects on the central segregation.

Figure 7 represents the central carbon segregation degrees of the billets with only TSR. Without TSR, the average and maximum central carbon segregation degrees are 1.16 and 1.28, respectively. With the increase in cooling intensity of TSR, the central segregation decreases. When the cooling intensity is 2.2 m^3 h^{-1}, the average central carbon segregation degree drops to a minimum value of 1.07. This value is higher than the minimum segregation of the billet when using only F-EMS. Therefore, it can be concluded that TSR is less effective than F-EMS on improving the central segregation under the current technological parameters. As TSR locates near the straightening position, excessive cooling of TSR may generate internal and surface cracks in the billet [27]. To control the cracks and consider the burden of the spraying system, the maximum cooling intensity of TSR is determined as 2.2 m^3 h^{-1}. If the cooling intensity exceeds this value, TSR may play a better effect on the central segregation.

6.2 Comparison on macro-morphologies

Figure 8 displays the macro-morphologies and rating of the billets under different conditions. There are no internal and surface cracks detected for the samples, which means that the current casting parameters can prevent the formation of cracks quite well. Without F-EMS or TSR, both the transverse and longitudinal samples exhibit bad compactness. On transverse sample, a slight central pipe and relatively severe central porosity are identified, which present serried black spots around the billet center. The grades of central porosity and pipe are about 2.0 and 2.0, respectively. Severe V-segregation is observed on the longitudinal sample, and it represents discrete black strips near the billet center and a long crevice at the centerline. By applying F-EMS or TSR, the central pipe, central porosity,
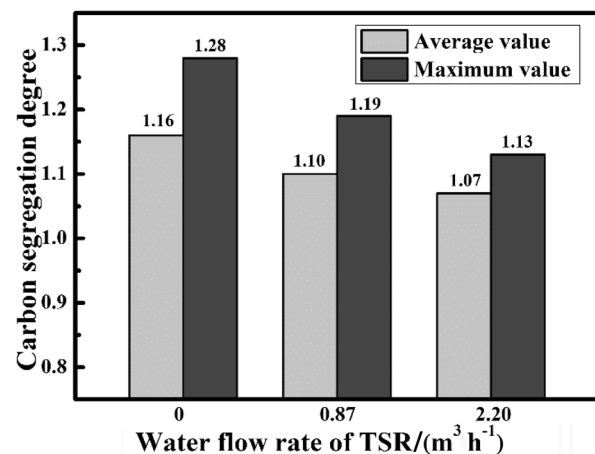

Fig. 7 Central carbon segregation degrees of billets with only TSR

	0 A, 0 m³/h	200 A, 0 m³/h	240 A, 0 m³/h	280 A, 0 m³/h	0 A, 0.87 m³/h	0 A, 2.2 m³/h
Transverse sample						
Longitudinal sample						
	○:2.0 ■:2.0	○:1.0 ■:1.0	○:1.0 ■:1.5	○:1.5 ■:1.0	○:1.0 ■:1.0	○:0.5 ■:1.0

○:Grade of central porosity ■:Grade of central pipe

Fig. 8 Macro-morphologies and rating of billets under different conditions

and V-segregation are visibly alleviated. Moreover, the effect of TSR is more prominent than that of F-EMS, especially for V-segregation. The grades of central porosity and pipe can drop to 0.5 and 1.0 when the water flow rate of TSR is 2.2 m³/h. The samples with only F-EMS still possess certain porosity, but the ones with only TSR show good compactness at the billet center, and the compactness improves with higher cooling intensity of TSR.

According to the results from Fig. 8, it can be obtained that TSR shows better improvement on V-segregation, central porosity, and pipe than F-EMS, which is opposite in the case of central segregation. These results can be explained by the different mechanisms of F-EMS and TSR on the billet. F-EMS has remarkable metallurgical effects, such as enhancing the liquid flow, homogenizing the temperature and solute elements of the liquid, breaking the dendrite, and increasing the central equiaxed crystal, which help in improving the central segregation. The enhanced liquid flow can improve the V-segregation by influencing the inflow of the liquid [28]. However, it also promotes the convective heat transfer of the residual liquid, which may increase the solidification shrinkage at the solidification end and in turn worsen the V-segregation, central porosity, and pipe. TSR can compensate the central solidification shrinkage through intensive water-spray cooling, and consequently, the inflow of enriched liquid can be inhibited [11], thus enhancing the improvement of V-segregation, central porosity, and pipe. The inhibition of the liquid inflow can also improve the central segregation, but its ability is limited as the uniformity of the residual liquid remains unchanged by TSR. Therefore, based on the comparison of F-EMS and TSR effects on the billet, it can be concluded that F-EMS is more helpful

in improving the central segregation, and TSR is prone to improve the V-segregation, central porosity, and pipe.

6.3 Integration of F-EMS and TSR

Figures 9 and 10 show the central carbon segregation degrees and macro-morphologies of the billets adopting the integrated process of F-EMS and TSR, respectively. It can be noted that the central carbon segregation degrees under different technological parameters differ greatly. When the cooling intensity of TSR is constant, the central segregation is also significantly affected by the current of F-EMS, where a medium current gives the minimum central segregation. This trend is consistent with the results shown in Fig. 6. From an overall perspective, it can be obtained that a high cooling intensity of TSR outperforms a lower one. The central segregation remains severe at a low cooling intensity of TSR and a small current of F-EMS. When the cooling intensity of TSR is 2.2 m³ h⁻¹, the central segregation at each F-EMS current is relatively low, and the average central carbon segregation degrees are controlled within 1.09. Since the coil of F-EMS may age and the spraying nozzles used for TSR may clog over time, the actual parameters of F-EMS and TSR may deviate from their optimum values, thus weakening their application effects. If F-EMS or TSR is fixed to their optimum parameters, the central segregation is generally steady when the parameters of the other technique change. Consequently, the integration of F-EMS and TSR is beneficial for central segregation stability. In terms of the macro morphologies, the samples show good compactness by the integration of F-EMS and TSR, and the V-segregation, central porosity, and pipe are slightly alleviated
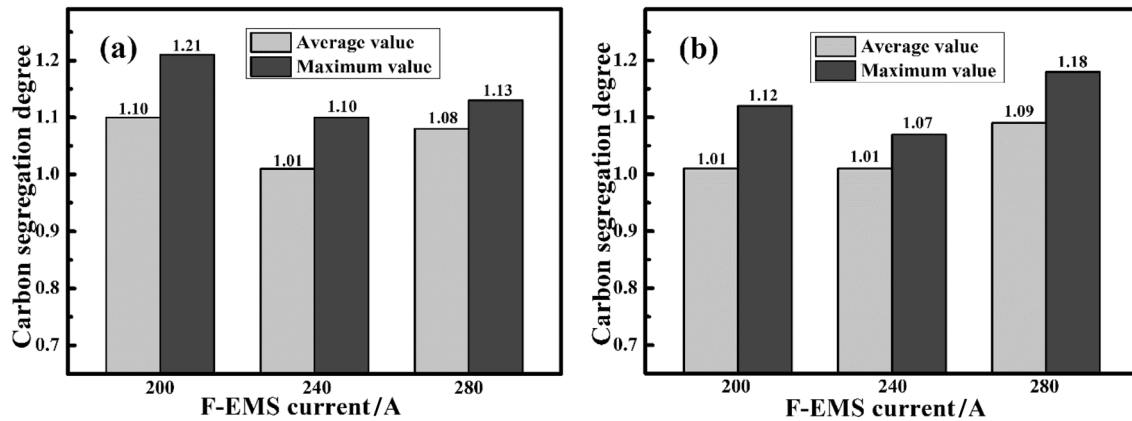
Fig. 9 Central carbon segregation degrees of billets with both F-EMS and TSR with cooling intensity of TSR of 0.87 m^3 h^{-1} (**a**) and 2.2 m^3 h^{-1} (**b**)
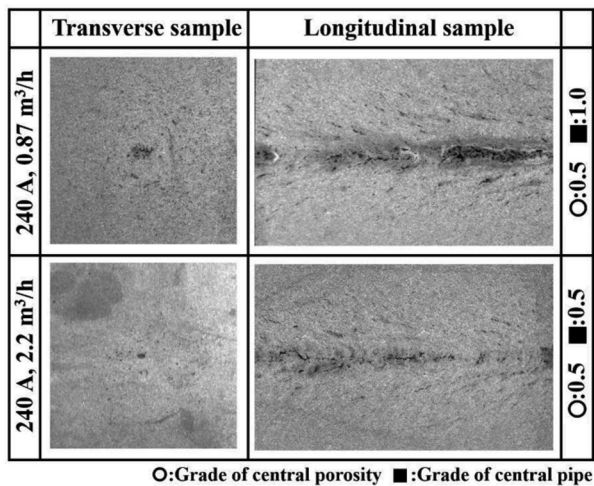

Fig. 10 Macro-morphologies and rating of billets with both F-EMS and TSR

compared to the samples with only F-EMS or TSR. The grades of central porosity and pipe can optimally drop to 0.5 and 0.5, respectively. In summary, the integration of F-EMS and TSR can utilize the advantages of each technique, and the billet could obtain an optimum inner quality when the current of F-EMS is 240 A and the cooling intensity of TSR is 2.2 m^3 h^{-1}.

7 Conclusions

1. The reasonable locations of F-EMS and TSR are determined to be at 6.63–7.23 m and 6.96–8.46 m from meniscus, respectively. The two techniques can be applied simultaneously, but F-EMS would need to be installed slightly before the initially determined position.

2. F-EMS or TSR can effectively improve the inner quality of the billet at their respective suitable working conditions. However, F-EMS is more helpful in terms of improving the central segregation, while TSR is prone to improve the V-segregation, central porosity, and pipe.

3. The integration of F-EMS and TSR can utilize the advantages of each technology and result in an optimal improvement of the inner quality of the billet. Among all the working conditions, 82A steel billet has an optimum inner quality when the current of F-EMS is 240 A and the cooling intensity of TSR is 2.2 m^3 h^{-1}.

References

[1] K. Liu, Q. Sun, J. Zhang, C. Wang, Metall. Res. Technol. 113 (2016) 504.

[2] Y. Chen, M.F. Xiao, G.R. Wu, J. Iron Steel Res. Int. 17 (2010) No. 6, 1–5.

[3] X. Zhao, J. Zhang, S. Lei, Y. Wang, Steel Res. Int. 85 (2014) 645–658.

[4] J.P. Zhao, L. Liu, W.W. Wang, W.J. Zhou, H. Lu, Ironmak. Steelmak. 46 (2019) 227–234.

[5] R. Wang, Y.P. Bao, Y.H. Li, H.H. An, Int. J. Miner. Metall. Mater. 23 (2016) 1150–1156.

[6] C. Xiao, J.M. Zhang, Y.Z. Luo, X.D. Wei, L. Wu, S.X. Wang, J. Iron Steel Res. Int. 20 (2013) No. 11, 13–20.

[7] J. Li, B. Wang, Y. Ma, J. Cui, Mater. Sci. Eng. A 425 (2006) 201–204.

[8] J. Zeng, W. Chen, S. Zhang, Y. Li, Q. Wang, ISIJ Int. 55 (2015) 2142–2149.

[9] P. Sivesson, G. Hallen, B. Widell, Ironmak. Steelmak. 25 (1998) 239.

[10] C.M. Raihle, P. Sivesson, M. Tukiainen, H. Fredriksson, Ironmak. Steelmak. 21 (1994) 487–495.

[11] P. Sivesson, C.M. Raihle, J. Konttinen, Mater. Sci. Eng. A 173 (1993) 299–304.

[12] J. Zeng, W. Chen, Q. Wang, G. Wang, Trans. Ind. Inst. Met. 69 (2016) 1623–1632.

[13] A. Scholes, Ironmak. Steelmak. 32 (2005) 101–108.

[14] H. An, Y.P. Bao, M. Wang, L.H. Zhao, Metall. Res. Technol. 114 (2017) 405.

[15] H. Sun, L. Li, J. Wang, X. Cheng, F. Zhou, Ironmak. Steelmak. 45 (2018) 708–713.

[16] A. Cristallini, A. Ferretti, R. Moretti, S. Simoni, in: Steelmaking Conf. Proc. 1994, pp. 309–315.

[17] Y. Han, X. Wang, J. Zhang, F. Zeng, J. Chen, M. Guan, Q. Liu, Metals 9 (2019) 543.

[18] Y. Han, W. Yan, J. Zhang, W. Chen, J. Chen, Q. Liu, ISIJ Int. 60 (2020) 106–113.

[19] G. Engstrom, H. Fredriksson, B. Rogberg, Scand. J. Metall. 12 (1983) 3–12.

[20] C.M. Raihle, H. Fredriksson, Metall. Mater. Trans. B 24 (1994) 123–133.

[21] H. Mizukami, M. Komatsu, T. Kitagawa, K. Kawakami, Tetsu-to-Hagane 70 (1984) 194–200.

[22] K.S. Oh, Y.W. Chang, ISIJ Int. 35 (1995) 866–875.

[23] D. Jiang, M. Zhu, Metall. Mater. Trans. B 48 (2017) 444–455.

[24] S. Luo, F.Y. Piao, D.B. Jiang, W.L. Wang, M.Y. Zhu, J. Iron Steel Res. Int. 21 (2014) 51–55.

[25] M.R. Bridge, G.D. Rogers, Metall. Trans. B 15 (1984) 581–589.

[26] S. Asai, N. Nishio, I. Muchi, Trans. Iron Steel Inst. Jpn. 22 (1982) 126–133.

[27] V. Ludlow, A. Normanton, A. Anderson, M. Thiele, J. Ciriza, J. Laraudogoitia, W. Van Der Knoop, Ironmak. Steelmak. 32 (2005) 68–74.

[28] J.J. Moore, N.A. Shah, Int. Met. Rev. 28 (1983) 336–356.